



## INELASTIC RESPONSES OF LONG BRIDGES TO ASYNCHRONOUS SEISMIC INPUTS

Jiachen WANG<sup>1</sup>, Athol CARR<sup>1</sup>, Nigel COOKE<sup>1</sup> and Peter MOSS<sup>1</sup>

### SUMMARY

The influence of two effects of the spatial variation of seismic ground motions, viz. the wave-passage effect and the geometric incoherence effect, on the inelastic responses of long bridges are considered in this paper. Analyses were carried out to produce time-history responses of long bridges with the seismic motions acting in the transverse direction of the bridge. The asynchronous seismic inputs were generated by using the conditional simulation method with a natural earthquake record specified at one abutment. Three different 3D bridge models and three different earthquake records were employed to determine the variation of bridge responses with the travelling wave velocity and the degree of the geometric incoherence. The results of these analyses show that the spatial variation of seismic ground motion significantly influences the response of long bridges. The responses of long bridges to asynchronous seismic inputs change with the travelling wave velocity and the degree of the geometric incoherence and they can be more critical than those under synchronous seismic inputs.

### INTRODUCTION

The effect of the spatial variation of the seismic ground motions on the response of extended structures was recognized a number of decades ago [1]. However, the spatial variability has only been attributed to the wave passage effect because of insufficient knowledge of the mechanisms underlying the spatial variability of the motion. In the case of the wave passage effect, it is assumed that the bridge response is solely due to the difference in arrival time at each support of an unmodified ground motion. A breakthrough occurred with the installation of the strong motion arrays and the analyses of the recorded data. Especially important was the data from SMART-1 array [2], which suggested that the seismic waves not only propagate on the ground surface, but they also change in shape at various locations. The change in shape of the ground motion results from reflections and refractions of waves through the soil and the superposition of the waves (the geometric incoherence effect). The difference in soil conditions at each support (the local site effect) modifies the amplitude and frequency of the waves. A wave dispersion factor 'd' is introduced into the calculations in order to take into account the local geological and topographical conditions. The larger the value of 'd', the greater the expected correlation between points of the random field that defines the ground motion i.e. less dispersion. This wave dispersion effect may also significantly

---

<sup>1</sup> Department of Civil Engineering, University of Canterbury, Christchurch, New Zealand.

influence the response of extended structures. Since the SMART-1 array has been in place, the spatial variability of the seismic ground motions and its effects on extended structures has attracted significant research interest. In this work, the dispersion introduced to the ground motion does not change the earthquake spectra.

In this paper, a study of the inelastic seismic response of long bridges with different configurations subjected to asynchronous input motions is described. The response parameters investigated were the maximum pier drifts, where ‘drift’ is defined as the deflection of the top of a pier relative to the base, the maximum pier shear forces and the maximum section curvature ratios of the piers. It was found that the asynchronous input motions had a significant effect on the response of these long bridges. The responses were dependent on the propagation velocity of the input motions when the geometric incoherence effect of the spatial variation of the seismic ground motions was least (when ‘d’ was large). As the effect of geometric incoherence increased, its influence on the total response of these long bridges increased. The total response became unpredictable for the cases with the greatest geometric incoherence effect (when ‘d’ was small).

### DESCRIPTION OF THE PROTOTYPE BRIDGE

The prototype bridge was a nine-span straight bridge continuous between abutments with a total length of 344m. The spans between the piers were 40m long while the end spans between the abutments and the adjacent pier are 32m long as shown in Figure 1. The deck was a twin box prestressed concrete girder and was supported on a single circular pier through sliding bearings and a cap beam. The bearings permitted longitudinal movement of the girder relative to the cap beam and shear keys restrained the transverse movement of the girder. Abutment 1 was constructed monolithically with the end diaphragm in the girder, and abutment 10 supported the girder-end through sliding bearings with freedom of movement longitudinally, transversely and rotationally.

The circular piers were reinforced concrete of 1.5m-diameter. A 2.5 m deep cap beam was monolithically connected to the top of each pier that had free heights of 6m, 8m, 5m, 5m, 5m, 11m, 11m and 5m for piers 2 to 9, respectively. The longitudinal reinforcement consisted of 48-32 mm diameter deformed bars in pairs running the entire height of the pier. The transverse reinforcement consisted of 12 mm diameter deformed bars at 75mm centers for the bottom 20% of the pier height and 140mm centers for the remainder of the height. The piers were supported by a 4.5m by 4.5m by 1.5m deep pile caps and four 1m-diameter piles. The design concrete cylinder strength was 35 MPa for the piers, and 45MPa for the prestressed girder. The nominal yield strength of the reinforcement was 430MPa. The site had uniform soil conditions, consisting of cohesionless soils.

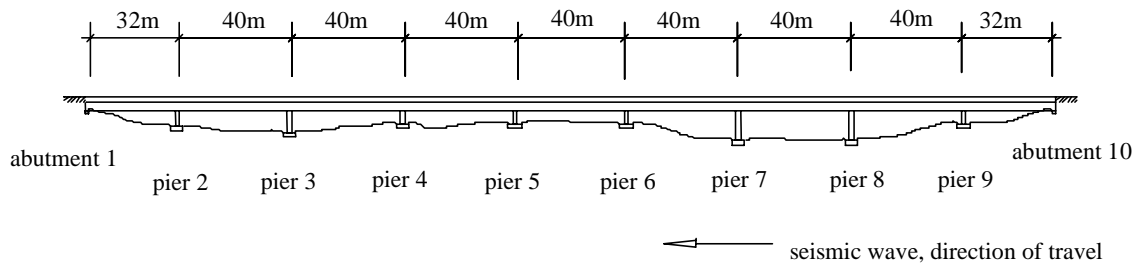


**Figure 1 Bridge elevation**

## STRUCTURAL MODELLING AND SEISMIC INPUT

The finite element model used in these analyses is shown in Figure 2. The girder was represented by three dimensional (3D) linear elastic beam members placed at the geometric centroid of the cross section, having the following characteristics:-

section area =  $6.93\text{m}^2$ ;      moments of inertia,  $I_{\max}=86.25\text{m}^4$  and  $I_{\min}=3.16\text{m}^4$ ;  
 torsional moment of inertia,  $J=6.97\text{m}^4$ ;      member length = 8m;      weight = 200kN/m.

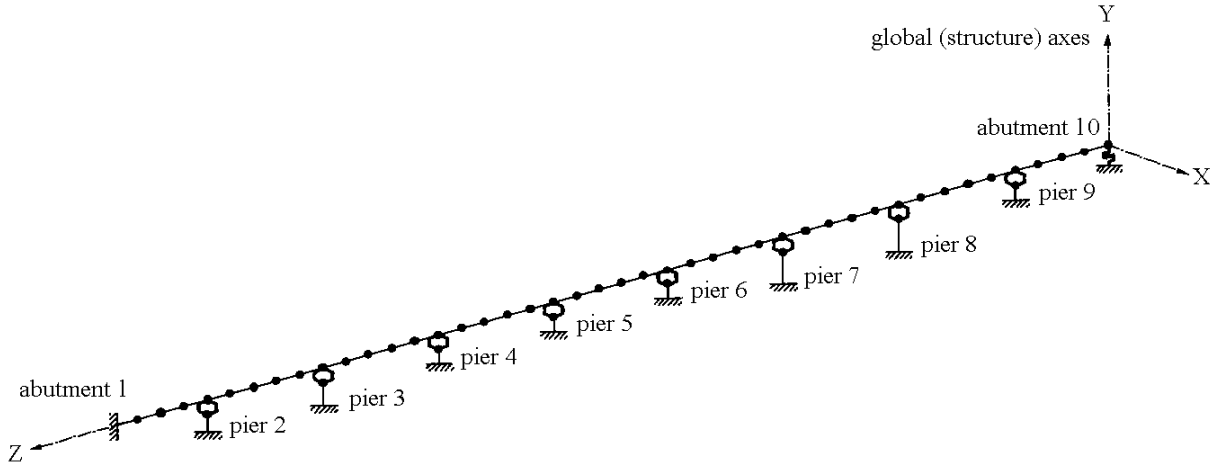


**Figure 2 General layout of the element model of bridge**

The piers were modeled as 3D concrete beam-column members using a one-component model by Carr [3], which idealized a reinforced concrete beam or column member as a perfectly elastic massless line element with non-linear rotational springs at the two ends to model the potential plastic hinges. The bi-linear hysteresis rule was employed for the hinge spring to represent the elastic and inelastic behavior of the member. The plastic hinge length  $L = D$  ( $D =$  the diameter of the piers) was assumed. The effective member properties, which reflected the extent of concrete cracking and reinforcement yielding, were taken as follows:

effective moment of inertia  $I_e=0.124\text{m}^4$ ; effective torsional moment of inertia  $J_e=0.15\text{m}^4$ ; effective shear area  $A_{ve}=0.88\text{m}^2$ .

The flexural rigidity  $EI_e$ , where  $E$  is elastic modulus and  $I_e$  is the effective second moment of area, was determined from section moment-curvature analyses as [4]:

$$EI_e = \frac{M_y}{\Phi_y} \quad (1)$$

where  $M_y$  and  $\Phi_y$  represent the ideal yield moment and curvature for a bilinear moment-curvature approximation. The result of the section moment-curvature analysis of the piers under a static axial load of 8MN is shown in Figure 3. The effective stiffness reduction in shear was considered proportional to the effective stiffness reduction in flexure [4]. The torsional moment of inertia was multiplied by a factor of 0.3 to get the effective torsional moment of inertia for these prototype bridge piers after Singh and Fenves [5]. Piers were assumed to be fixed at ground level i.e. at the top of the pile caps.

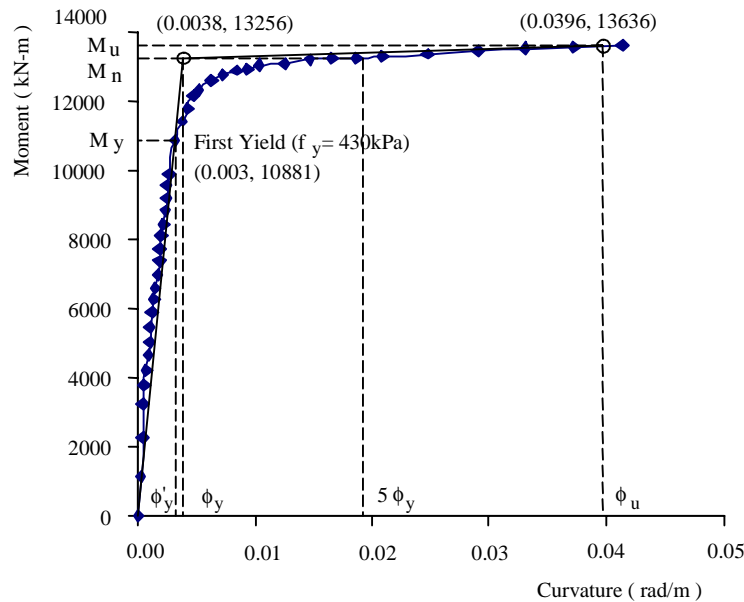


**Figure 3 Moment-curvature relationship for pier section**

Sliding bearings were modeled by 3D spring elements. The spring stiffness in the longitudinal direction was based on the idealized shearing deformation of the bearing pads given by  $G_{\text{elast}}A/h$  where  $G_{\text{elast}}=1.0\text{MPa}$  was the assumed shear modulus for the elastomer,  $h=50\text{mm}$  was the height of the bearing pads, and  $A=0.34\text{m}^2$  was the plan area of the bearing pads. The yield force was equal to the constant vertical reaction of the bearing pads from gravity loads multiplied by the dynamic friction coefficient of 0.12. For the bearings installed on the piers, the spring stiffness in the transverse direction was set as large as possible because the shear keys provide a rigid constraint in this direction. The bearings on the abutment 10 were given the same stiffness value in both the longitudinal and transverse directions.

Masses were lumped at the ends of each member. The Rayleigh damping model was used to model the damping exhibited by the structure in which the fractions of critical damping were assumed to be five percent in modes 1 and 2.

In order to enable conclusions to be drawn that were less structure-specific, three bridge models with different configurations were analyzed. Table 1 lists the characteristics of the configurations of the three bridge models.

For the asynchronous input motions, a natural earthquake record was specified at Abutment 10 and the conditionally simulated time-histories were used at pier supports and Abutment 1. It was assumed that the seismic input motions acted in the transverse direction of the bridge and propagated from Abutment 10 to Abutment 1 in the longitudinal direction. The seismic time-histories were generated using the simple method for stochastic dispersion of earthquake waves [6]. The cases, in which the combined geometric incoherence and wave passage effects were considered, are referred to as wave dispersion cases in the sections that follow. Three natural earthquake records, the El Centro 1940 and the Northridge 1994 NS components and one from the Mexico City 1985 earthquake, were employed at Abutment 10 respectively as the specified earthquake motion.

**Table 1 The description of bridge models (see Figure 1)**

	The free heights of piers	Boundary conditions
Model 1	6m, 8m, 5m, 5m, 5m, 11m, 11m, 5m for piers 2 to 9	At abutment 1 the superstructure was completely fixed while at abutment 10 the superstructure was supported on the abutment structure through sliding bearings (vertical support only)
Model 2	11m for all piers	At abutment 1 and abutment 10 the superstructure was supported on the abutment structure through sliding bearings (vertical support only)
Model 3	5m for all piers	Same as model 2

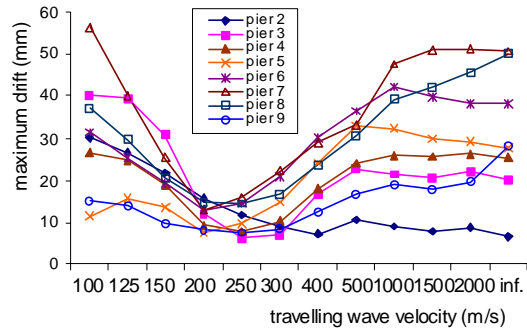
### **THE SEISMIC RESPONSE OF BRIDGE MODEL 1**

The responses of Model 1 subjected to the NS component of the El Centro 1940 earthquake record with an input scale factor of 0.5 at Abutment 10 and the generated time-histories at other piers and Abutment 1 are shown in Figure 4. For the cases with the least dispersion ( $d = 100$ ), the variations of the maximum pier drifts with the travelling wave velocity (Figure 4 (b)) followed similar trends to those in the wave-passage effect only cases (Figure 4(a)) [7]. However, the corresponding values of the maximum pier drift in these wave dispersion cases and the wave passage cases were slightly different and these differences increased for piers 2 and 3 which were adjacent to the fixed abutment..

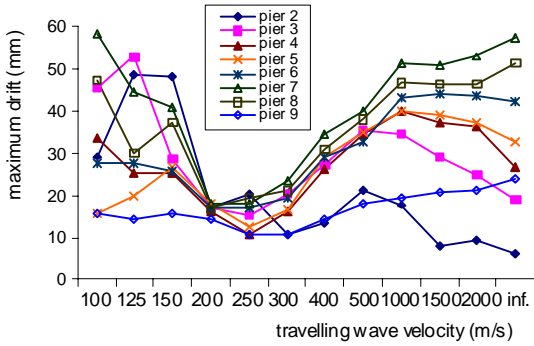
For the cases with the greatest dispersion ( $d = 1$ ), the variations of the maximum pier drifts with the travelling wave velocity (Figure 4 (e)) did not follow any observable trend and were very different from the wave passage cases. The drifts for the dispersion cases were mostly much greater (maximum of 420mm) than for the wave passage cases (maximum of 58mm).

The results for the cases with a dispersion factor of 50 and 10 showed a mixed behavior. When the travelling wave velocity was greater than 400m/s for  $d = 50$  and 1000m/s for  $d = 10$ , the response varied with the traveling wave velocity in a similar way as the wave-passage effect cases. However, when the traveling wave velocity was less than these values, there was not any noticeable trend (see Figures 4(c) and 4(d)). The differences in response between the wave dispersion and the wave passage cases increased with increase in dispersion i.e. decrease in wave dispersion factor 'd'.

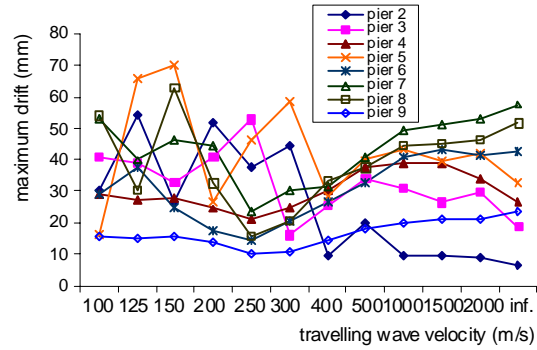
The variations in maximum pier section curvature ratios and maximum pier shear forces with travelling wave velocity were similar to the drift response [8]. The variations in maximum pier section curvature ratios with traveling wave velocity are shown in Figure 5. Large inelastic section curvature demands in Figure 5 are associated with the large drifts in Figure 4.



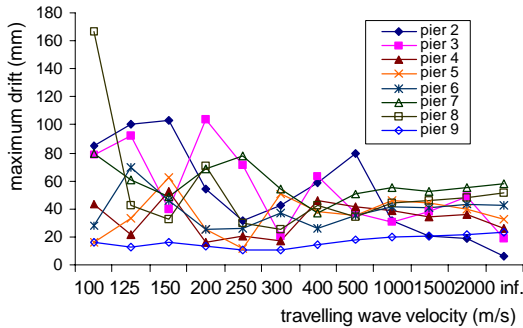
(a) wave passage effect only (no dispersion)



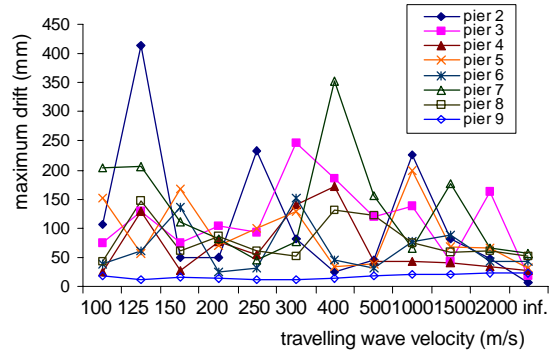
(b) wave dispersion factor  $d = 100$



(c) wave dispersion factor  $d = 50$



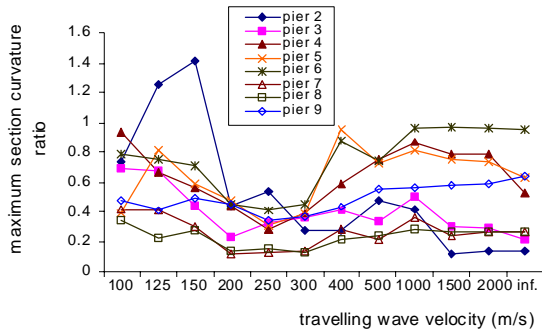
(d) wave dispersion factor  $d = 10$



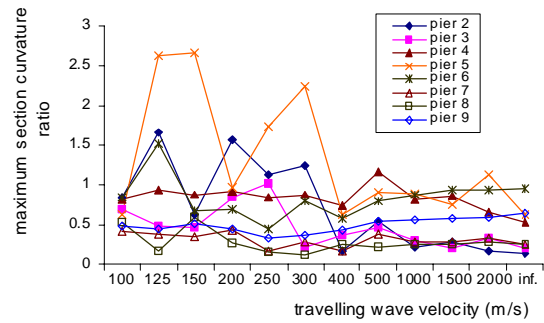
(e) wave dispersion factor  $d = 1$

**Figure 4 The maximum drifts of Model 1 to EL40NSC with an input scale factor of 0.5.**

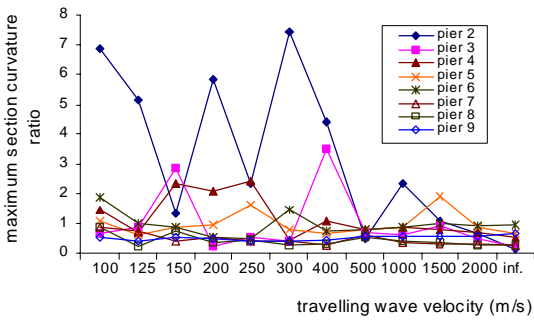
Similar observations were made for the variations of the maximum pier drifts, the maximum section curvature ratios of the piers and the maximum pier shear forces with traveling wave velocity when Model 1 was subjected to other earthquakes. The other earthquakes used in these analyses are the North-South component of the Northridge 1994 earthquake record, with input scale factor of 0.15, and the Mexico City 1985 earthquake with input scale factor of 0.5 [8]. The drift response to the Mexico City earthquake for the wave passage effect is shown in Figure 6 and similarly the variations of the maximum pier drifts with traveling wave velocity to the NS component of Northridge 1994 earthquake record are shown in Figure 7.



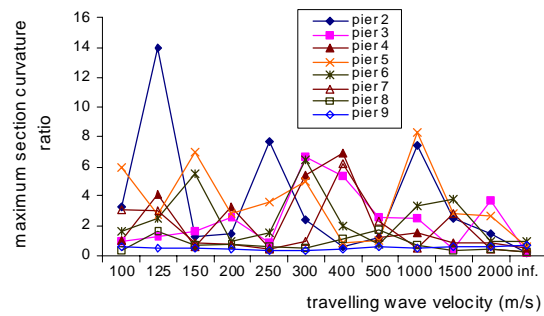
(a) dispersion factor  $d = 100$



(b) dispersion factor  $d = 50$



(c) dispersion factor  $d = 10$



(d) dispersion factor  $d = 1$

**Figure 5 The maximum section curvature ratios of Model 1 to EL40NSC with input scale factor of 0.5**

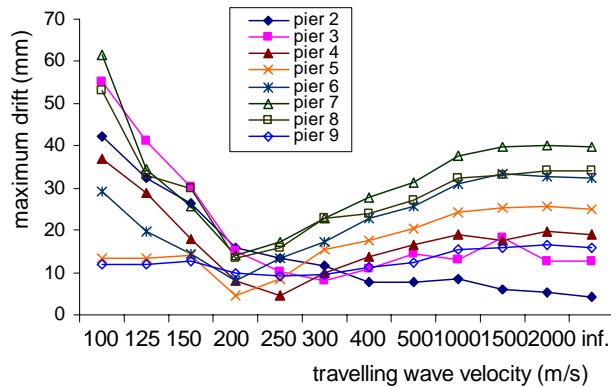
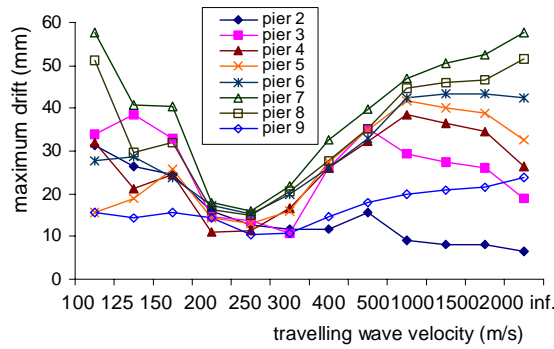
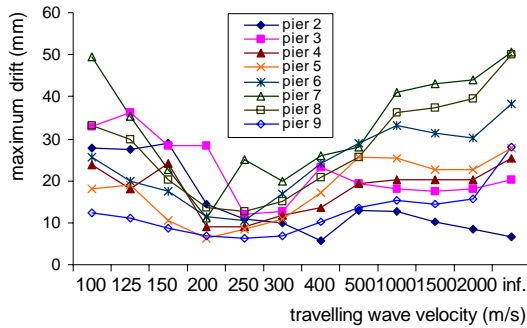


**Figure 6 The maximum drifts of Model 1 to MEXSCT1L with an input scale factor of 0.5.**

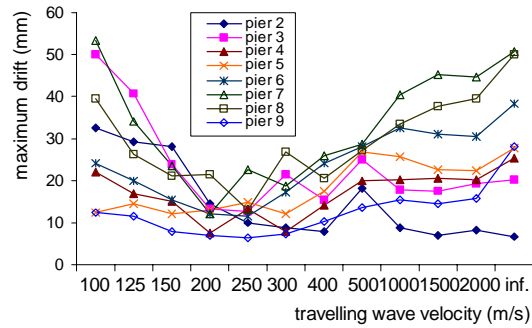
The response of long bridges to asynchronous input motions consists of two components [9], a dynamic component induced by the inertia forces and a pseudo-static component due to the difference between the adjacent support displacements. The dynamic components of the responses showed insignificant differences between the wave dispersion cases and the wave passage effect cases because their acceleration spectra at different supports were almost identical, following the rule adopted in the



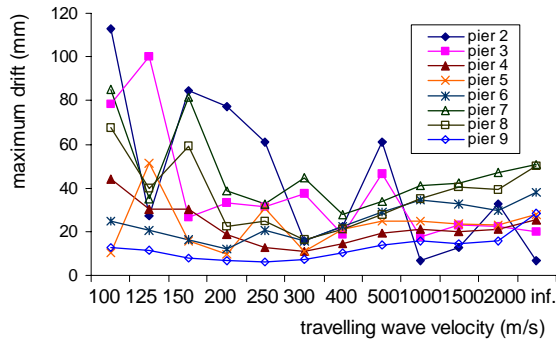
(a) wave passage effect only



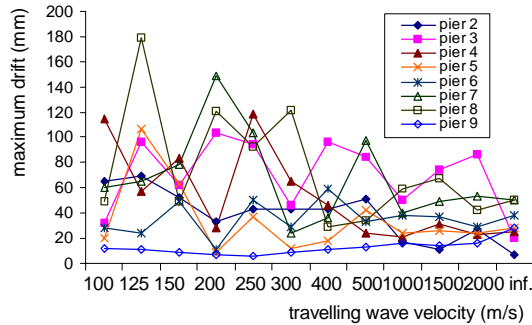
(b) wave dispersion factor  $d = 100$



(c) wave dispersion factor  $d = 50$



(d) wave dispersion factor  $d = 10$

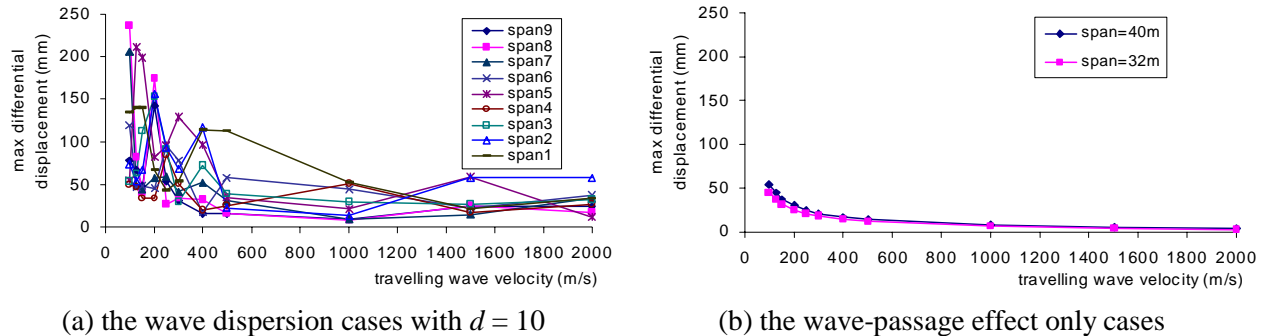


(e) wave dispersion factor  $d = 1$

**Figure 7 The maximum drifts of Model 1 to SYLM949 with an input scale factor of 0.15.**

generation of the seismic motions. Any differences in the total responses between the wave dispersion cases and the wave-passage effect cases can be attributed to the differences in the pseudo-static components. In the wave dispersion cases the pseudo-static component consists of two parts resulting from the geometric incoherence effect and wave passage effect. Although the changes in the accelerograms between the adjacent supports were very small, the differential displacements between the adjacent supports caused by these changes are not necessarily small, resulting in additional stresses in the structure. Figure 8(a) shows the maximum differential displacements between the adjacent supports in Model 1 in the wave dispersion cases with  $d = 10$  and the El Centro 1940 earthquake record. Figure 8(b) shows the corresponding responses for the wave-passage effect cases [7]. It can be seen that the

differential displacements between the adjacent supports caused by the wave dispersion effect were generally larger than those caused by the wave passage effect, which is nearly a lower bound to the results in Figure 8(a). It follows that the pseudo-static component due to the geometric incoherence effect could be more important than that caused by the wave passage effect as the dispersion factor decreases. Furthermore, the differential displacements between the adjacent supports caused by the geometric incoherence effect used in these analyses are random and are therefore unpredictable so the pseudo-static component caused by the geometric incoherence effect will also be unpredictable.



(a) the wave dispersion cases with  $d = 10$  (b) the wave-passage effect only cases  
**Figure 8 Maximum differential displacements between pier bases in Model 1 (EL40NSC with an input scale factor of 0.5)**

Comparing the responses of the wave dispersion cases with the corresponding responses for the wave-passage effect only cases of Model 1 [7], it also is noticeable that when the geometric incoherence effect and wave passage effect are considered together the responses are generally larger than those reached when only the wave passage effect is taken into account. The maximum pier drifts increase with the decrease of the dispersion factor 'd' i.e. increasing dispersion. This indicates that the pseudo-static component caused by the geometric incoherence effect has a very significant influence on the total response in the wave dispersion cases and this influence increases considerably with the decrease of the dispersion factor. Furthermore, in the wave-passage effect only cases, all the piers remain elastic when the input scale factor of 0.5 is used for the input seismic motion of the El Centro 1940 earthquake NS component record, but some piers behave inelastically in the wave dispersion cases even for the cases with  $d = 100$  and the maximum section curvature of the piers [8] and the maximum pier shear forces also increase considerably with the decrease of the dispersion factor (Figure 5).

### THE SEISMIC RESPONSE OF OTHER BRIDGE MODELS

Despite the fact that the bridge Models 2 and 3 had very different configurations from Model 1, the variations of the maximum pier drifts (see Figure 9 for Model 2 drifts), the maximum section curvature ratios of the piers and the maximum pier shear forces with the traveling wave velocity had very similar trends to that observed in the wave dispersion cases for Model 1 [8]. For the cases with least dispersion ( $d = 100$ ), the variations of the responses with the traveling wave velocity were very similar to those cases where only the wave-passage effect was considered. For the cases with the greatest dispersion ( $d = 1$ ), the variations of the responses with the traveling wave velocity did not follow any noticeable trend. For the cases with a dispersion factor of 10, the results showed a mixed behavior. When the traveling wave velocity was greater than 1000m/s the variations of the maximum pier drifts with the traveling wave velocity followed similar trends to those in the wave-passage effect cases, but when the traveling wave velocity was less than 1000m/s the variations of the maximum pier drifts with the traveling wave velocity

did not follow any observable trend. The maximum drift responses of Model 2 subjected to the El Centro 1940 NS earthquake component with an input scale factor of 1, are shown in Figure 9.

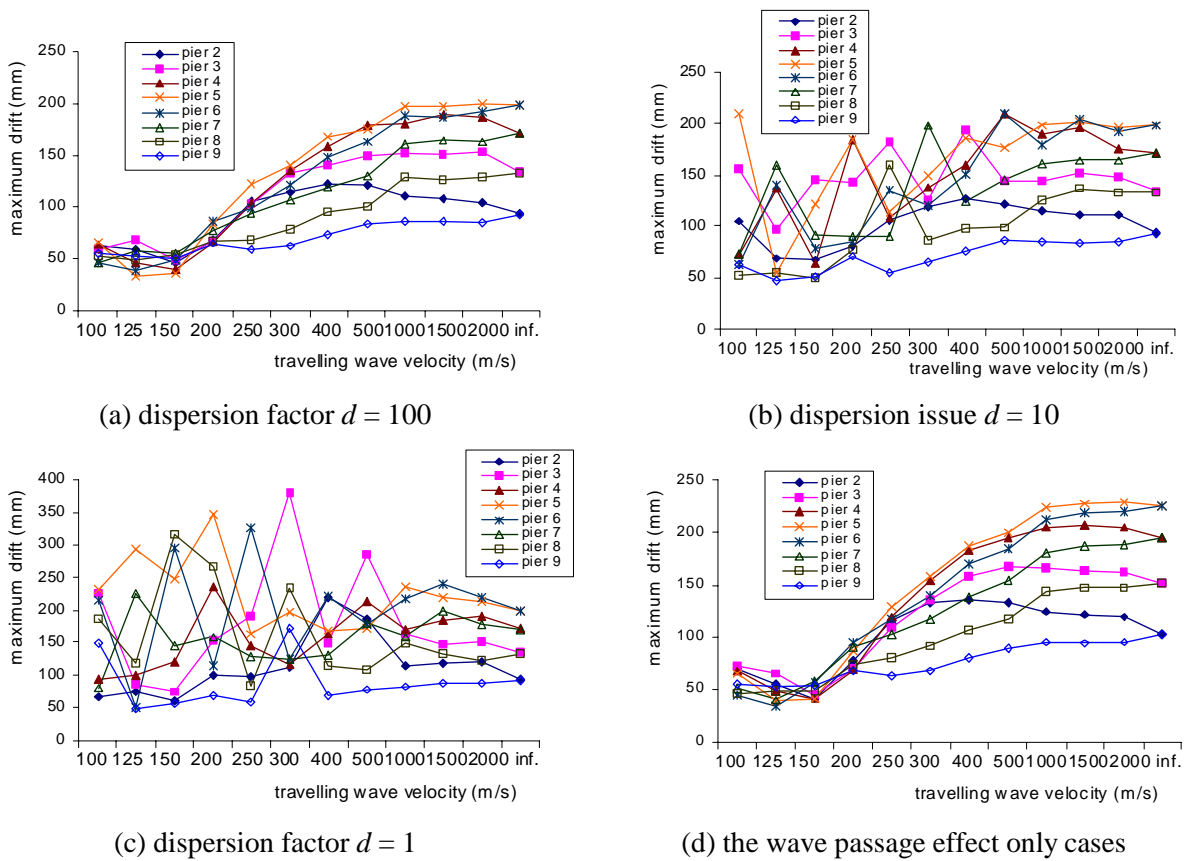


**Figure 9 The maximum drifts of Model 2 to EL40NSC with input scale factor of 1.0.**

## CONCLUSIONS

It was found that the asynchronous input motions had a significant effect on the response of the long bridges and the responses to asynchronous inputs could be more serious than those from synchronous inputs.

The response of long bridges was dependent on the propagation velocity of the input ground motions for the wave passage effect.

When the geometric incoherence effect of the spatial variation of the seismic ground motions was small i.e.  $d=100$ , the response was similar to the wave passage cases. As the geometric incoherence effect increased, its influence on response increased. For example, at  $d=50$ , velocities less than 400m/s were influenced; at  $d=10$  this had increased to velocities less than 1000m/s and at  $d=1$ , all responses had become unpredictable.

Pier drift, pier shear force and pier section curvature response for the three different long bridges modeled were very similar.

Responses to the three earthquake components were very similar.

### ACKNOWLEDGEMENT

The doctoral scholarship provided by University of Canterbury to the first author is gratefully acknowledged.

### REFERENCES

1. Bogdanoff, J. L., J. E. Goldberg, and A. J. Schiff. 1965. "The effect of Ground Transmission Time on the Response of Long Structures." *Bulletin of the Seismological Society of America*, Vol. 55 (No. 3), 627-640.
2. Abrahamson, N. A., et al. (1987). "The SMART-1 Accelerograph Array (1980-1987): A Review." *Earthquake Spectra*, Vol. 3 (No. 2).
3. Carr, A. J. 2001. "RUAUMOKO 3D." Department of Civil Engineering, University of Canterbury, Christchurch, New Zealand.
4. Priestley, M. J. N., F. Seible, and G. M. Calvi. 1996. *Seismic Design and Retrofit of Bridges*, John Wiley & Sons, Inc.
5. Singh, S. P., and G. L. Fenves, 1994. "Earthquake Response of 'Structure A' Using Nonlinear Dynamic Analysis", in *Seismic Design and Retrofitting of Reinforced Concrete Bridges* R. Park(ed.), Proceedings of the Second International Workshop held in Queenstown, New Zealand.
6. Wang, J, A. Carr, N. Cooke and P. Moss, 2003a. "A simple method for stochastic dispersion of earthquake waves" Proceedings of 2003 Pacific Conference on Earthquake Engineering, Christchurch, New Zealand
7. Wang, J, A. Carr, N. Cooke and P. Moss, 2003b. "Wave-passage effect on the seismic response of long bridges" Proceedings of 2003 Pacific Conference on Earthquake Engineering, Christchurch, New Zealand.
8. Wang, J 2003 "Analysis Of The Seismic Response Of Highway Bridges To Multiple Support Excitations" Ph.D thesis, Department of Civil Engineering, University of Canterbury, Christchurch, New Zealand.
9. Clough, R. W., and J. Penzien. 1993. *Dynamics of Structures*, McGraw-Hill, New York.